Liquid Crystals
Publication details, including instructions for authors and subscription information:
http://www.informaworld.com/smpp/title~content=t713926090

Surface ordering at the air-nematic interface. Part 1. A neutron reflection study of translational order

Y. G. J. Lau[ab]; R. M. Richardson[b]; R. M. Dalgliesh[c]; H. Zimmermann[d]
[a] Institut Laue-Langevin, Cedex 9, France [b] H. H. Wills Physics Laboratory, Royal Fort, Bristol BS8 1TL, UK [c] ISIS Rutherford Appleton Laboratory, Chilton, Didcot, Oxon, OX11 0QX, UK [d] Max-Planck-Insititut fur Medizinische Forschung, 69120 Heidelberg, Germany

To cite this Article Lau, Y. G. J. , Richardson, R. M. , Dalgliesh, R. M. and Zimmermann, H.(2007) 'Surface ordering at the air-nematic interface. Part 1. A neutron reflection study of translational order', Liquid Crystals, 34: 3, 333 — 341
To link to this Article: DOI: 10.1080/02678290601116316
URL: http://dx.doi.org/10.1080/02678290601116316

Liquid Crystals, Vol. 34, No. 3, March 2007, 333–341

Surface ordering at the air–nematic interface. Part 1. A neutron reflection study of translational order

Y. G. J. LAU†‡, R. M. RICHARDSON*‡, R. M. DALGLIESH§ and H. ZIMMERMANN¶

†Institut Laue-Langevin, 6 Rue Jules Horowitz, BP 156 – 38042 Grenoble, Cedex 9, France
‡H. H. Wills Physics Laboratory, Royal Fort, Tyndall Avenue, Bristol BS8 1TL, UK
§ISIS Rutherford Appleton Laboratory, Chilton, Didcot, Oxon, OX11 0QX, UK
¶Max-Planck-Insititut fur Medizinische Forschung, Jahnstrasse 29, 69120 Heidelberg, Germany

(*Received 19 May 2006; accepted 6 September 2006*)

Neutron reflection was used to measure the build-up of layers at the air surface as the smectic phase was approached from higher temperatures in a nematic liquid crystal. The liquid crystal was 4-octyl-4′-cyanobiphenyl with a deuterated core and hydrogenous tails. The development of surface smectic layers in the nematic phase was followed by measuring specular reflectivity and monitoring the pseudo-Bragg peak from the layers. The pseudo-Bragg peak therefore corresponded to the formation of long-range smectic layers at the surface as the transition temperature is approached. The results were consistent with the continuous growth of smectic layers at the surface and the amplitude of the smectic density wave decayed with increasing distance from the surface. The depth over which the smectic layering occurred at the interface was found to be ~450 Å at a quarter of a degree above the nematic to smectic A bulk transition. The smectic order parameter at the surface was ~0.1 which is much less that found for typical homeotropic alignment agents.

1. Introduction

There has been considerable interest in the use of X-ray reflection in the last two decades to study structural phenomena at liquid crystal surfaces [1, 2]. The technique is useful for obtaining information at the molecular level perpendicular to an interface. The formation of smectic layers at the air–liquid crystal interface has been studied using X-ray reflection [1]. It was found that at the surface, the director tended to be perpendicular to the surface and that there was a strong tendency for the smectic layers to form at temperatures for which the bulk of the material remained in the nematic or isotropic phase. It has been demonstrated that surface and bulk scattering can be separated in such measurements, and that values of the bulk and surface critical correlations lengths can be determined in a single reflection measurement. These results provided structural information on liquid crystals at the air interface as well as giving an interesting insight to the field of phase transitions and critical phenomena. An X-ray reflection experiment conducted at the air–liquid crystal interface with an added dopant was also carried out [2] but due to lack of contrast between the dopant and host liquid crystal, observations of changes of surface order in the liquid crystal were inconclusive. Therefore, a motivation for using neutrons to look at the air–liquid crystal interface is the possibility of using isotopic substitution to optimize scattering contrast in the single- or many-component system. Neutrons are particularly suitable for this since the neutron scattering lengths of hydrogen and deuterium are different ($b_H = -3.30$ fm and $b_D = 6.67$ fm). Isotopic substitution between H and D therefore allows the possibility of large contrast variations in scattering length density (SLD) without altering the physical and chemical properties of the sample. This H/D substitution is therefore ideal for contrasting different organic materials.

The aim of the experiment reported here is to explore the feasibility of neutron reflection from the air–nematic interface with a view to extending to multicomponent systems in future. In this work, a partially deuterated liquid crystal was used in order to improve the signal from smectic layering at the interface relative to the background from incoherent scattering.

2. Theoretical summary

In a reflection experiment, the neutron beam is incident at a surface in the $z=0$ plane at an angle θ to the surface. The neutron reflectivity from such a surface may be

*Corresponding author. Email: Robert.richardson@bristol.ac.uk

Liquid Crystals
ISSN 0267-8292 print/ISSN 1366-5855 online © 2007 Taylor & Francis
http://www.tandf.co.uk/journals
DOI: 10.1080/02678290601116316

divided into two parts. The specular reflection has a scattering vector, **Q**, perpendicular to the surface, i.e. $Q=Q_z$, $Q_x=Q_y=0$, and contains information on the refractive index for neutrons in a direction normal to the surface. If the surface is invariant in the x- and y-directions it gives only specular reflection. If the surface is structured in the x- or y-directions then there will be some off-specular scattering, i.e. reflected intensity with Q_x or $Q_y \neq 0$. Off-specular scattering may also be given by inhomogeneity in the bulk phase. The variation of neutron refractive index with distance is simply related to the SLD so that measurement of specular reflection provides information on the structure of the surface in a direction perpendicular to the interface.

One of the most convenient ways of calculating reflectivity is using the matrix formulism of classical optics. This formulism is based on an arbitrary stratification of the medium by a series of uniform strata [3] where each stratum is characterized by a scattering length density and a thickness. This method shall be used in the present work to calculate reflectivity.

In this paper, specular neutron reflection [4] from the air–liquid crystal surface has been measured and analysed. There are two distinct surface phenomena in liquid crystals [5]. One is the discrete film of smectic layers at the surface and the other is a gradual enhancement of smectic layers as the surface is approached. These two types can also be characterized in terms of wetting phenomena at first order phase transitions [6]. The first type has been observed in liquid crystals with direct isotropic–smectic A transitions [7], whereas the latter type has been seen in liquid crystals with a bulk nematic phase [1]. The surface transitions are highly dependent on the properties of the interface and there has been theoretical research in this area [5, 6]. The models [8] for reflectivity for these two types of surface smectic order will now be described. In both models the density profile at the nematic air interface was modelled as an error function with a standard deviation, σ_1. Within the liquid crystal, the density profile (and hence the SLD profile) of a surface-induced smectic phase can be described by a sinusoidal wave. If the smectic region is formed by discrete addition of layers, the sine wave is truncated at some finite distance from the interface. The wave is defined by its maximum amplitude, ρ_1, the smectic layer period, d, the phase φ of the wave, the thickness of the smectic region at the interface, ξ_s, and the mean scattering length density of the bulk nematic, ρ_0. The SLD on the nematic side of the interface, $\rho^+(z)$, for the discrete layering model is then given a function of depth, z, by the equation

$$\rho^+(z) = \rho_0 + \rho_1 \sin\left(\frac{2\pi z}{d} + \varphi\right)\left[\frac{1}{2} - \frac{1}{2}\mathrm{erf}(\xi_s, \sigma_2)\right] \quad (1)$$

where $\mathrm{erf}(\xi_s, \sigma_2)$ is an error function centred at position ξ_s and with standard deviation, σ_2. The decay of the sine wave can take place over any distance between one smectic layer spacing, i.e. $\sigma_2=d$ corresponding to a uniform surface film, and a distance equal to the actual thickness of the surface film, i.e. $\sigma_2=\xi_s$ corresponding to a more diffuse interface with the bulk. These profiles are expected when step-wise growth (layer by layer) of the smectic film occurs.

The density profile for a diffuse surface smectic film can also be described by a sinusoidal density wave as above, but instead of terminating at some distance from the surface, the wave decays exponentially into the bulk phase. This profile is expected for films that grow continuously rather than in the form of a wetting film. The same parameters ρ_1, d and φ are used to describe the sine wave, but now ξ_s represents the exponential decay length of the smectic order away from the interface. The scattering length density within the liquid crystal phase $\rho^+(z)$ as a function of z for the continuous layering model is then given by

$$\rho^+(z) = \rho_0 + \rho_1 \sin\left(\frac{2\pi z}{d} + \varphi\right)\exp\left(\frac{-z}{\xi_s}\right). \quad (2)$$

Note that the truncated model with $\sigma_2=\xi_s$ is similar to the exponential decay but differs slightly in that it a convex function. Figure 1 shows the reflectivities and scattering length densities as calculated using Abelès matrix formulism for the uniform film model, and figure 2 shows the reflectivities and scattering length densities for the continuous model. The two models have distinguishable reflectivity profiles. In the uniform film model, fringes appear on either side of the pseudo-Bragg peak and become more prominent with increasing number of smectic layers. Fringes are not present in the reflectivity of the exponential decay model for any surface decay length, ξ_s, but the peak is broader at its base.

The parameters in these SLD models may be linked to other physical quantities. Since a smectic A layer is not polar, it is convenient to describe the structure in terms of 'dimers' consisting of pairs of antiparallel molecules. The mean SLD, ρ_0, is determined by the number density of 8CB dimers, n_0, and the scattering lengths of the N atoms of one molecule,

$$\rho_0 = 2n_0 \sum_{i=1}^{N} b_i. \quad (3)$$

The maximum amplitude of the SLD wave, ρ_1, is

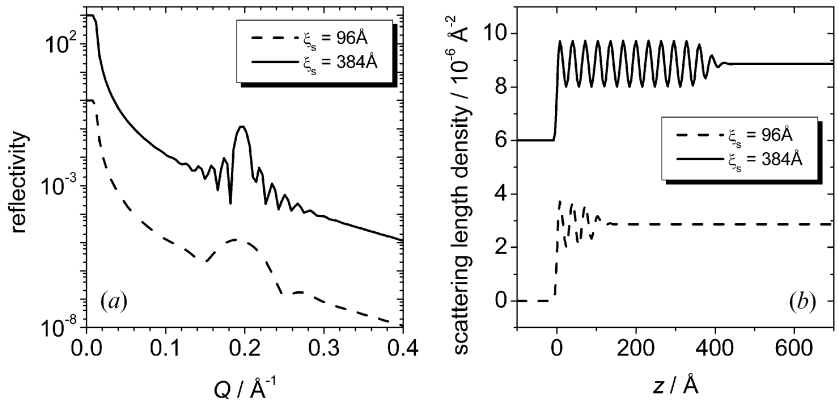

Figure 1. (a) Reflectivity calculated using the discrete layering model with $\xi_s=d$; (b) the respective scattering length density profiles. (Note that the solid line has been shifted for clarity).

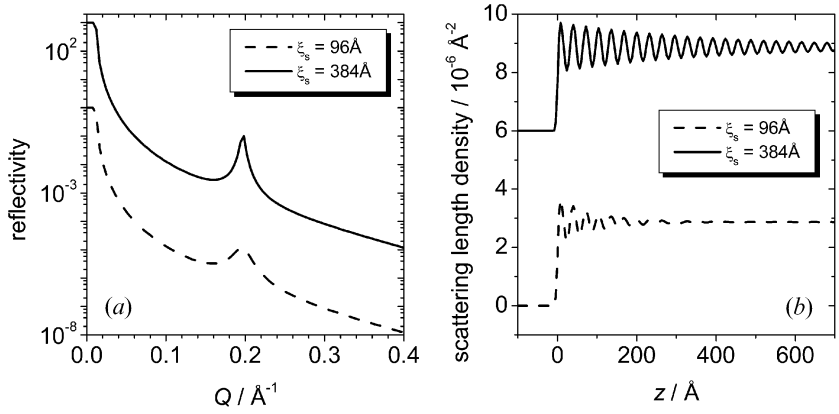

Figure 2. (a) Reflectivity calculated using the continuous layering model; (b) the respective scattering length density profiles. (Note that the solid line has been shifted for clarity).

determined by the maximum amplitude of the sinusoidal number density wave, n_1, of the dimers and the distance, a_i, of the atoms in the molecule from the centre of the layer, such that

$$\rho_1 = 2n_1 f' \tag{4}$$

where $f' = \sum b_i \cos(2\pi a_i/d)$. These formulae are also valid for X-ray reflection where the scattering length, b, would be the atomic number multiplied by the Thompson scattering length of an electron. A detailed derivation is presented elsewhere [8]. Since the maximum smectic order parameter is determined by n_0 and n_1, the surface smectic order parameter, τ_s, can be calculated as

$$\tau_s = \langle \cos\left(\frac{2\pi z}{d}\right) \rangle = \frac{n_1}{2n_0} \tag{5}$$

where the angle brackets indicate average over $n(z)$. It is possible to determine τ_s from the experimental values of ρ_0 and ρ_1 from equation (2) as

$$\tau_s = \frac{\rho_1}{2\rho_0} f \tag{6}$$

where $f = \sum b_i/f'$. It has been shown that in smectic phases of cyanobiphenyls the cores of two molecules overlap with the alkyl tails pointing in opposite directions to form a 'dimer'. For 8CB the layer spacing d is about 1.4 times the length of a single molecule [9]. By assuming dimer structure, the factor f may be calculated and, the surface smectic order parameter τ_s can then be calculated from the value of ρ_1 that is determined from specular reflectivity measurements using equation (6). The value of f depends on the conformational structure of the 8CB dimer used but it has been shown in previous work [8] that the sensitivity is rather low. Here, it is assumed that the molecular tilt angle from the layer normal is zero. The coordinates of a molecule of 8CB in a reasonably linear conformation were generated by Cerius^{2}® [10] and were placed with

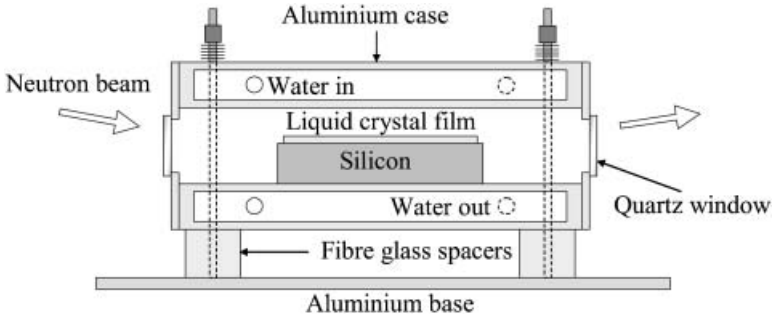

Figure 3. The constant temperature sample enclosure with liquid crystal film on top of a rough silicon block.

the principal axis of inertia perpendicular to the layer. This molecule was then rotated by 180° and shifted to generate the second molecule such that the two molecules overlapped with a total length equal to the smectic *d*-spacing.

The smectic adsorption parameter, $\Gamma(\tau)$, has been introduced from theory [5] as a convenient way to characterize the smectic layer formation at surfaces. For a lattice theory this surface adsorption is given by

$$\Gamma(\tau) = \frac{1}{\tau(T_{AN})} \sum_m \tau_m \tag{7}$$

where τ_m is the smectic order parameter in layer m counting from the surface and $\tau(T_{NA})$ is the bulk value at the N–SmA transition. This absorption parameter may also be calculated [8] from experimentally determined parameters: τ_s, ξ_s and d provided τ_b, the bulk order parameter of the smectic phase just below the transition, is known. For 8CB, this is found to be τ_b=0.43 [9].

$$\Gamma(\tau) \cong \frac{\tau_s}{\tau_b} \frac{\xi_s}{d}. \tag{8}$$

3. Experimental method

A core-deuterated liquid crystal, 4-octyl-4′-cyanobiphenyl (8CB-d_8), was synthesized using previously published methods [11]. Its isotopic purity was found to be >99% by NMR. A film of 8CB-d_8 (~0.5 g) was placed on top of a rough silicon disc (100 mm diameter). The silicon disc was placed inside a constant temperature enclosure where the temperature was controlled by an external water bath. Fused quartz windows fixed onto either side of the temperature box allowed entry and exit of the neutron beam. This apparatus is shown in figure 3.

The reflection measurements were made using the CRISP reflectometer at the ISIS facility (UK). The CRISP reflectometer was chosen because it has an inclined incident beam and is therefore suitable for fluid interfaces. It is described elsewhere [12]. An incident angle of 2.2° was used so that the maximum intensity occurred at $Q_z \sim 0.2\,\text{Å}^{-1}$ where the pseudo-Bragg peak was expected to develop. A measurement of reflectivity from the bare air–silicon interface showed that there was no specular scattering from this rough surface; it was then assumed that scattering from this interface did not contribute to the final reflectivity. Reflectivity from the air–8CB-d_8 interface was measured at a series of temperatures starting in the isotropic phase through to the smectic phase. In order to extract true specular reflectivity from the surface, the bulk scattering from short-range smectic correlations in the nematic bulk [13] that gives rise to off-specular scattering had to be subtracted. A position-sensitive detector allowed the simultaneous measurement of specular, background and off-specular scattering from the sample. A typical data set is shown in figure 4 at T–T_{NA}=0.75°C, where T_{NA} is the nematic–smectic A (N–SmA) transition temperature. Standard corrections including that for the incident beam spectrum have been applied. The wavelength λ is calculated from the arrival time of the neutrons at the detector, and the angle θ is determined by the position of the beam on the detector, therefore Q_x and Q_z can be determined. In the two-dimensional map of intensity vs. θ and λ, the specular reflectivity is seen at a constant θ value that corresponds to Q_x=0 and the off-specular scattering from smectic fluctuations in the bulk is seen as a broad sloping peak that corresponds to constant Q_z. Since the information about the surface smectic layers is only contained in the specular reflectivity, it is essential to subtract the background due to incoherent scattering and bulk scattering. The specular reflectivity was extracted from the data in the θ–λ form in order to avoid errors in interpolating data to a regular Q_x–Q_z grid. Normal practice involves interpolating background from regions on either side of the specular ridge at constant λ. Unfortunately this method is inadequate for removing background scattering that is highly structured and

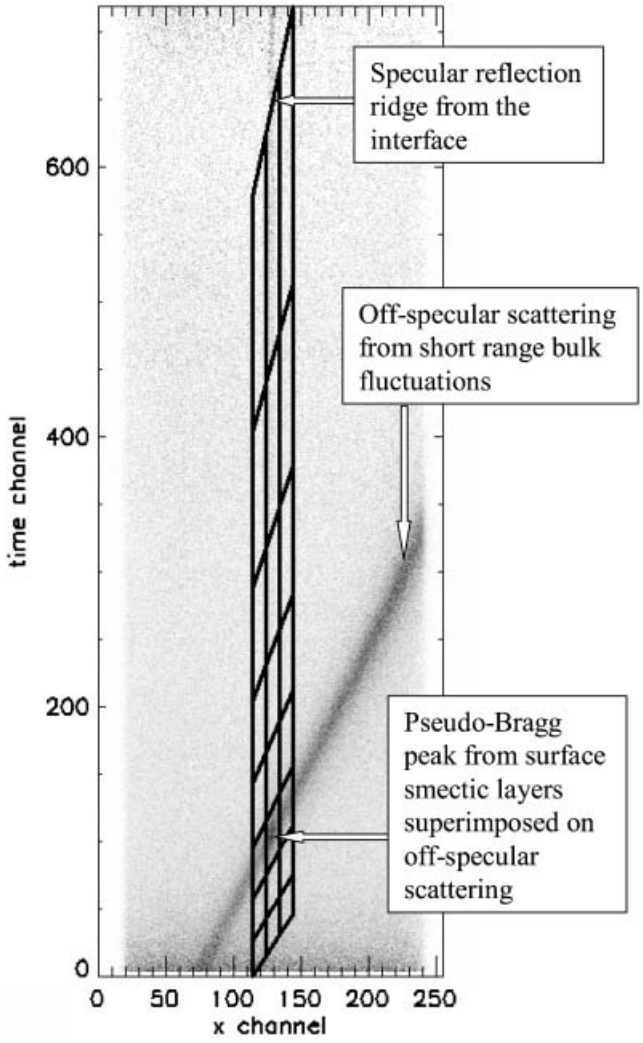

Figure 4. Reflectivity from the sample at $T-T_{NA}=0.75^{\circ}$C. The vertical axis represents the time of arrival of the neutrons which increased with neutron wavelength λ, and the horizontal axis represents the position at which the neutrons arrive at the detector which decrease with scattered angle θ. The specular part is seen at a constant θ angle which translates to $Q_x=0$ in Q, and the off-specular part contributes to scattering with constant $Q_z \sim Q_0$ in Q but not constant λ in this plot. The number of boxes used in data reduction is actually eight times more than that illustrated here.

which varies strongly with λ such as the off-specular scattering shown in figure 4. So, the specular reflectivity was divided into boxes in the central specular strip as shown in figure 4. The boxes are such that the Q_z-step is constant. The counts in each box were summed. The background was interpolated from adjacent boxes on either side of the specular strip but at the same Q_z (instead of at the same λ) and subtracted from the sum. The errors were calculated from the statistics of the total counts in each box. In this way, the incoherent background and off-specular scattering from smectic fluctuations in the bulk nematic were eliminated to leave true specular reflectivity. This contains the required information on the long range smectic layers at the surface.

4. Results and discussion

Figure 5a shows the shows reflectivity for 0.75°C above the transition temperature, T_{NA}, which was determined by a large jump in the reflected intensity. The reflectivity consists of a $\sim Q^{-4}$ decay and a pseudo-Bragg peak at $Q \sim 0.2\,\text{Å}^{-1}$ from the surface smectic layers. The exponential decay model, equation (2), and the truncation models — equation (1) with $\sigma_2=d$, $\xi_s/2$, and ξ_s — were fitted to the data at all temperatures. The best fits were obtained with the exponential decay model and the truncation model with $\sigma_2=\xi_s$ because the others showed side fringes to the peak which were not present in the data. The fit qualities for these two models were indistinguishable by visual inspection or using a quality of fit (χ^2) criterion and since their SLD profiles are so similar, the subsequent analysis will be reported for the exponential model only.

The data in figure 5 have been fitted by the exponential model with the phase angle φ fixed at values between -90° and $+215^{\circ}$. The amplitude ρ_1, layer spacing d and surface correlation length ξ_s were allowed to vary and the mean scattering length density ρ_0 was fixed at a value of $2.87\times10^{-6}\,\text{Å}^{-2}$ for 8CB-d_8. The roughness of the air–8CB-d_8 interface, σ_1, had been determined to be 6 ± 2 Å by fitting to the isotropic phase data (at $T-T_{NA}=14.5^{\circ}$C) and was fixed for all other temperatures. The scale factor (to convert the intensity to reflectivity) was also determined by fitting to the isotropic phase data. Figure 5b shows the corresponding scattering length density profiles.

From figure 5a, it can be seen that some phase angles give better fits to reflectivity than others. This is because the pseudo-Bragg peak in the model is slightly skewed to the left for $\varphi=-90^{\circ}$, slightly skewed to the right for $\varphi=+90^{\circ}$ and symmetric for $\varphi=0$ or 180°. Phase angles $\varphi=0$ and 180° appear to give the best fits since the peak in the data is reasonably symmetric. This is confirmed by figure 6 which shows plots of reduced χ^2 for the fits at each of the temperatures for each of the phase angles. The fits with $\varphi=0^{\circ}$ and $\varphi=+180^{\circ}$ give the lowest reduced χ^2. This is in contrast to recent solid-liquid crystal interface results at homeotropically aligned surfaces where only a phase angle of $\varphi=-90^{\circ}$ could be used to fit the data [8]. Physically, a phase angle of $\varphi=-90^{\circ}$ would mean that the first layer at the surface will consist of a full smectic dimer with the chains on the outside of the dimer and the cores on the inside of the layer. A phase angle of $\varphi=+90^{\circ}$ on the other hand suggests that it is the

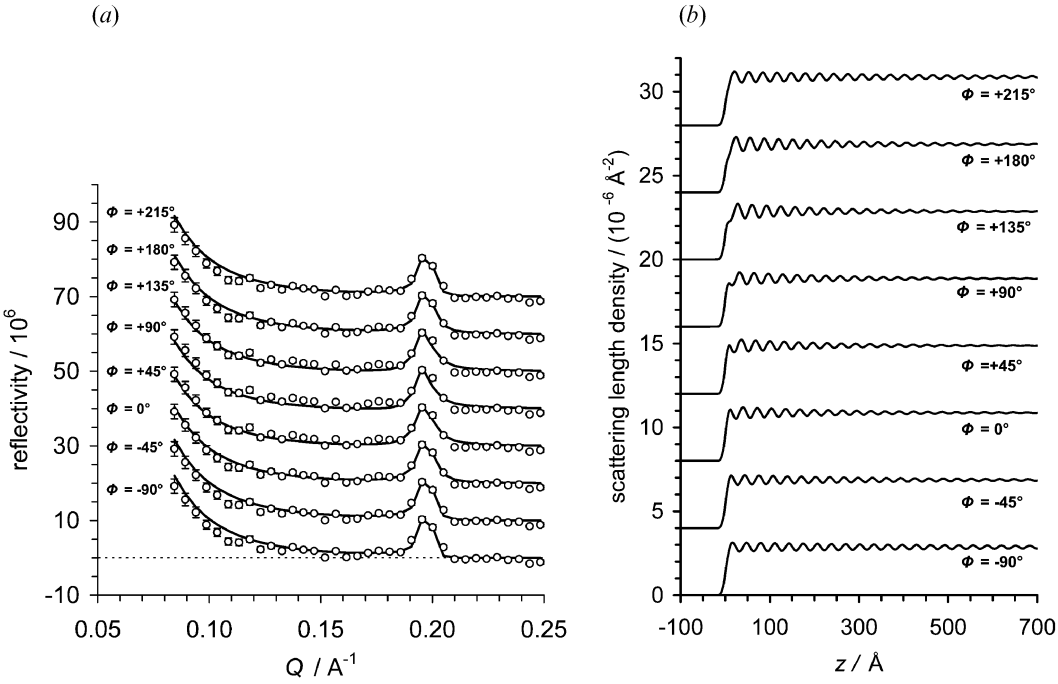

Figure 5. (a) Reflectivity at T–T_{NA}=0.75°C with fits with different fixed values of the phase angle; (b) the corresponding scattering length density profiles.

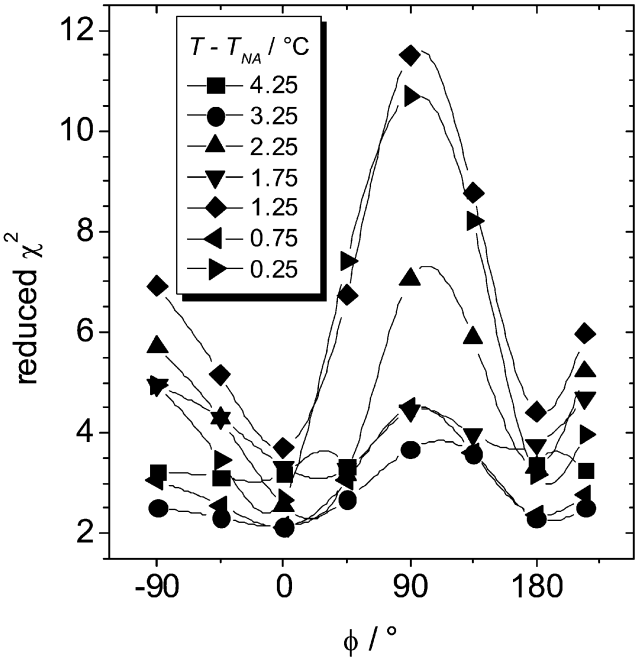

Figure 6. Plot of reduced χ^2 to fits using a different phase angle φ at each of the reduced temperatures. The lines are drawn to guide the eye.

cores that are at the surface. Other angles would suggest an anomalous smectic layer at the surface.

Figure 7 shows the scattering length density profiles for $\varphi=-90^\circ$ and $+90^\circ$ with illustrations of 8CB layer structure. Profiles for other possible values of φ, such as 0° and 180°, are not illustrated because they imply an anomalous first layer (i.e. a monolayer rather than partial bilayer). There are several possible structures for such a layer but choosing one for an illustration would imply a preference that cannot be substantiated at this stage. Since the deuterated aromatic core of the 8CB molecule has the highest scattering length, its position should correspond to the maximum. At present, the air–liquid crystal interface data presents two possible surface structures, each one giving rise to a different value of the surface smectic order parameter which will be outlined later.

Using equation (6), the surface smectic order parameter was calculated using parameters found in the best fits with $\varphi=0$ and $+180^\circ$. Figure 8 shows the results as a function of reduced temperature as the open points. The model with $\varphi=0^\circ$ gives a lower order parameter at $\tau_s\sim0.1$ which is independent of temperature. The model with $\varphi=+180^\circ$ gives $\tau_s\sim0.15$ but increasing with temperature which seems physically unreasonable. To try to distinguish between these two possibilities experimentally, a parallel set of measurements was made using X-ray reflection. The data were obtained using a Phillips X'Pert Pro X-ray diffraction system. The results also showed a pseudo-Bragg peak as T_{NA} was approached from higher temperatures. While similar analyses could not distinguish between φ values using the quality of the fit criterion (χ^2), there was good

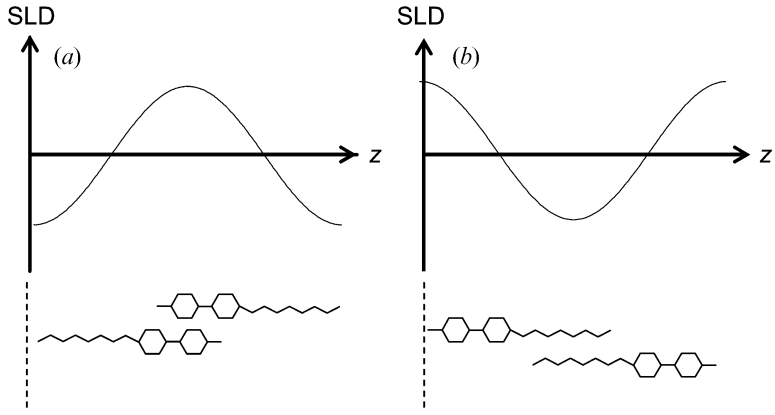

Figure 7. The scattering length density profiles for (a) $\varphi=-90^\circ$ and (b) $\varphi=+90^\circ$ with illustrations of 8CB layer structure.

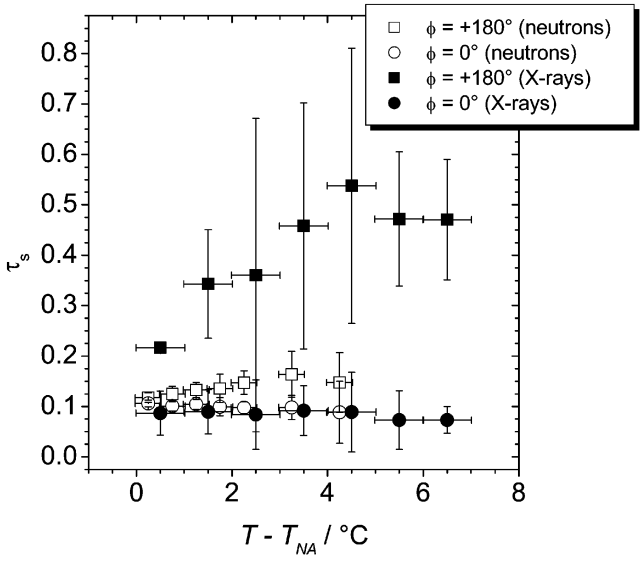

Figure 8. Surface smectic order parameter τ_s as function of T–T_{NA} for phase angles $\varphi=0$ and $+180^\circ$ from X-ray and neutron reflection data.

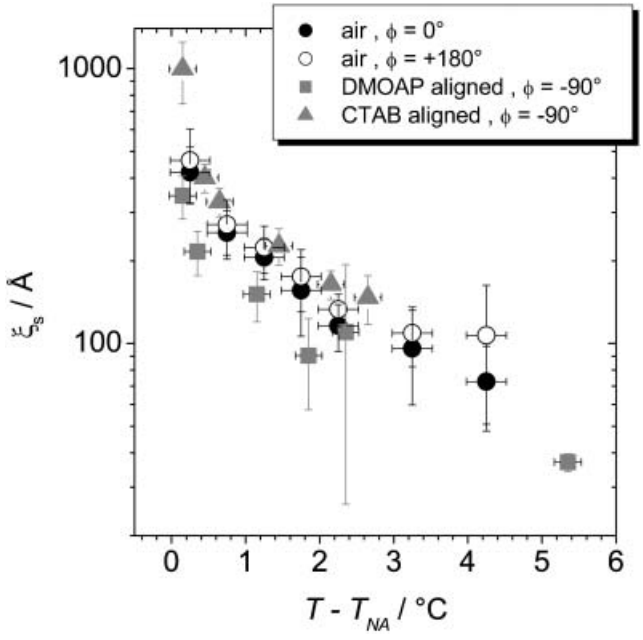

Figure 9. Surface decay lengths ξ_s found at the air interface and at the solid interface for homeotropic alignment using different surface treatments [8].

agreement with the neutron reflection values of τ_s if $\varphi=0^\circ$ was assumed but not if $\varphi=+180^\circ$ was assumed. Hence the solution using $\varphi=0^\circ$ is preferred. The results for τ_s using X-rays are shown as shaded points in figure 8 together with the neutron results as open points. The value of $\tau_s\sim0.1$ is significantly less that has been found for nematics in contact with homeotropic alignment agents [8]. For instance CTAB gave $\tau_s\sim0.5$ and other materials gave $\tau_s\sim0.3$.

The decay length ξ_s increased from about 80 Å four degrees above the transition to about 450 Å at one quarter of a degree above. The values of the decay lengths were found to be comparable to the lengths found at a solid substrate with certain homeotropic alignment treatments, with lengths intermediate between that of CTAB and DMOAP [8]. The results for ξ_s from reflectivity data at the solid–liquid crystal interface aligned with DMOAP and CTAB are shown in figure 9 alongside the air–interface data for phase angles $\varphi=0^\circ$ and $+180^\circ$. The plots confirm that the influence of the surface does extend well beyond the first layer of molecules as found previously for different surface treatments at the solid substrate.

The decay length ξ_s is expected to show a power law divergence similar to the bulk smectic correlation length [1]. This power law takes the form

$$\xi \sim t_c^{-\nu} \tag{9}$$

where t_c is the reduced temperate $t_c=(T-T_{NA})/T_c$, T_c is

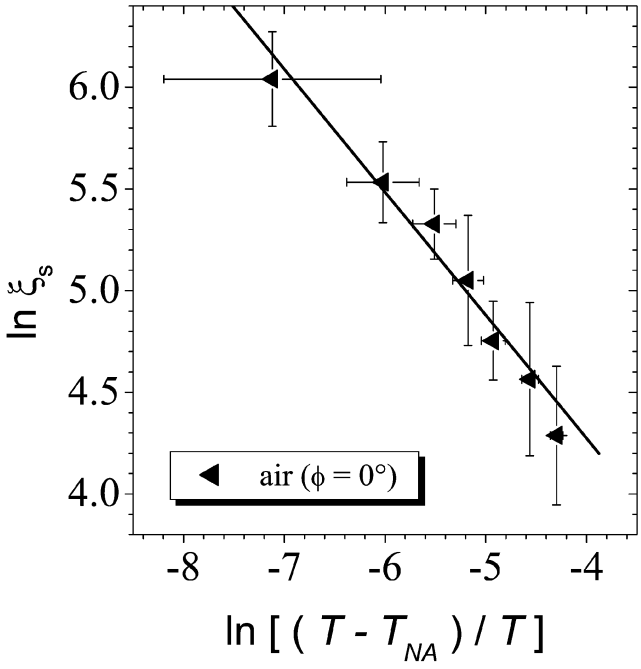

Figure 10. Log–log plot of surface decay length, ξ_s, as a function of reduced temperature $t=(T–T_{NA})/T$ with straight line fit. The line is $\ln(\xi_s/\text{Å})=(1.85\pm0.61)–(0.61\pm0.11)\ln t$.

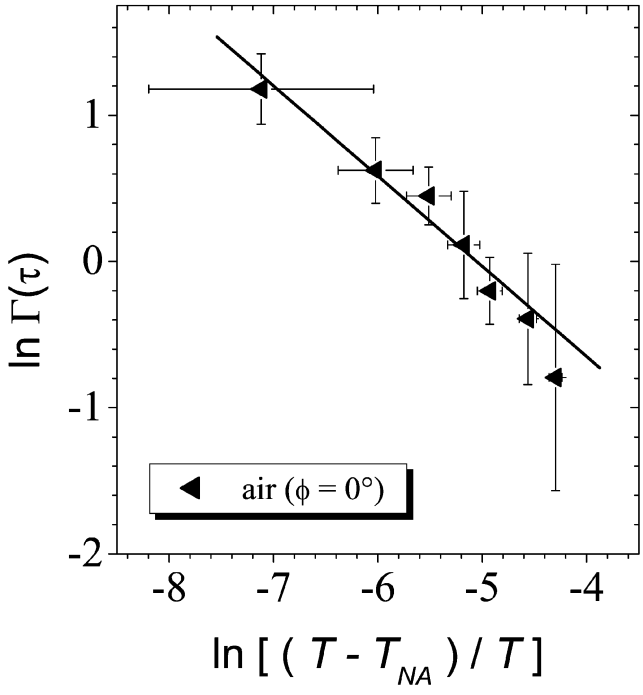

Figure 11. Log–log plot of the smectic adsorption parameter $\Gamma(T)$ vs. $t=(T–T_{NA})/T$ and straight line fit. The line is $\ln(\Gamma)=(3.12\pm0.73)–(0.62\pm0.13)\ln t$.

the transition temperature and ν is the critical exponent for the correlation length. Although thermodynamic functions are usually much more complicated than the formula in equation (9) with many other terms, the leading term is accurate near the phase transition. The result is that log–log plots can be used in order to determine the critical exponent ν. For this experiment, the reduced temperature $t=(T–T_{NA})/T$ was used rather than t_c because the experiment probes temperatures far from the transition hence extrapolating the temperature using T rather T_c is much more accurate over this temperature range [14]. Figure 10 shows plots for $\ln\xi(t)$ vs. $\ln t$ for the model where $\varphi=0^\circ$. The surface critical exponent was fitted using nonlinear least squares weighted by error (ignoring error in $\ln t$). The value found was $\nu=0.61\pm0.11$.

It is expected that Γ will also show a power law divergence with temperature as $\Gamma(\tau, t)\sim t^{-\beta}$. Log–log plots of $\Gamma(\tau)$ vs. t are shown in figure 11. A linear least squares fit to the data weighted by error (ignoring errors in $\ln t$) gives the value of the critical exponent, $\beta=0.62\pm0.12$. This value of β agrees within error with the value of $\beta\sim0.56$ that found for several solid–liquid crystal interfaces [8].

5. Conclusion

In conclusion, neutron reflectivity has been shown to be a useful technique for determining interfacial structure at a free nematic surface. The results show that smectic order at the free surface is less than at a strongly homeotropically aligning solid surface but that the extent of layering, as identified by the decay lengths, is similar. It shows that the influence of the surface extends well beyond the first layer of molecules. The surface smectic phase also grows continuously as the temperature is lowered and appears to diverge at the nematic–smectic A transition. This is as expected for second order or weakly first order phase transitions.

In the immediate vicinity of the air interface, it appears that there is no normal partial bilayer next to the surface. Confirmation of this suggestion will be sought by further isotopic substitutions of the liquid crystal molecule such that the phase angle and near surface structure can be established more accurately.

These neutron reflection results will also be compared with measurements at the air–liquid crystal interface using ellipsometric techniques where the probe couples with the refractive indices of the liquid crystal rather than with the mass density wave. Information on surface enhanced orientational order can thus be determined. These investigations will be published in a separate paper.

It has been established that reflection measurements have good sensitivity to the presence of smectic layering at the air–liquid crystal interface, and these experiments pave the way for studies looking at the disruption or

enhancement of surface-induced smectic order in mixtures.

Acknowledgements

R. M. R. and Y. G. J. L. would like to thank the ISIS facility for neutron beam time.

References

[1] P.S. Pershan, A. Braslau, A.H. Weiss, J. Als-Nielson. *Phys. Rev. A*, **35**, 4800 (1987).
[2] G.J. Kellogg, P.S. Pershan, E.H. Kawamoto, W.F. Foster, M. Deutsch, B.M. Ocko. *Phys. Rev. E*, **51**, 4709 (1995).
[3] F. Abelès. *Annls. Phys. (Paris)*, **5**, 596 (1950).
[4] J. Penfold, R.K. Thomas. *J. Phys. condensed Matter*, **2**, 1369 (1990).
[5] Z. Pawlowska, T.J. Sluckin, G.F. Kventsel. *Phys. Rev. A*, **38**, 5342 (1988).
[6] A.M. Somoza, L. Mederos, D.E. Sullivan. *Phys. Rev. Lett.*, **72**, 3674 (1994).
[7] B.M. Ocko. *Phys. Rev. Lett.*, **64**, 2160 (1990).
[8] Y.G.J. Lau, R.M. Richardson, R. Cubitt. *J. chem. Phys.*, **124**, 234910 (2006).
[9] A.J. Leadbetter, J.C. Frost, J.P. Gaughan. *J. Phys.*, **40**, 375 (1979).
[10] Information on Cerius^{2}® from Accelrys can be found online at http://www.accelrys.com/products/cerius2.
[11] H. Zimmermann. *Liq. Cryst.*, **4**, 591 (1989).
[12] J. Penfold. *Physica B*, **173**, 1 (1991).
[13] P.G. de Gennes, J. Prost. *The Physics of Liquid Crystals*. Oxford University Press, Oxford (2003).
[14] J. Als-Nielson. In *Phase Transitions and Critical Phenomena*, Vol. 5a, C. Domb, M.S. Green (Eds), Academic Press, London (1976).